



HAL
open science

1/f Tunnel Current Noise through Si-bound Alkyl Monolayers

Nicolas Clement, Stephane Pleutin, Oliver Seitz, Stephane Lenfant,
Dominique Vuillaume

► **To cite this version:**

Nicolas Clement, Stephane Pleutin, Oliver Seitz, Stephane Lenfant, Dominique Vuillaume. 1/f Tunnel Current Noise through Si-bound Alkyl Monolayers. 2007. hal-00125398v1

HAL Id: hal-00125398

<https://hal.science/hal-00125398v1>

Preprint submitted on 19 Jan 2007 (v1), last revised 29 Sep 2007 (v3)

HAL is a multi-disciplinary open access archive for the deposit and dissemination of scientific research documents, whether they are published or not. The documents may come from teaching and research institutions in France or abroad, or from public or private research centers.

L'archive ouverte pluridisciplinaire **HAL**, est destinée au dépôt et à la diffusion de documents scientifiques de niveau recherche, publiés ou non, émanant des établissements d'enseignement et de recherche français ou étrangers, des laboratoires publics ou privés.

$1/f^\gamma$ Tunnel Current Noise through Si-bound Alkyl Monolayers

Nicolas Clément¹, Stéphane Pleutin¹, Oliver Seitz², Stéphane Lenfant¹ and Dominique Vuillaume^{1,a}

¹ "Molecular Nanostructures and Devices" group, Institute for Electronics, Microelectronics and Nanotechnology, CNRS, BP60069, Avenue Poincaré, F-59652 cedex, Villeneuve d'Ascq, France

² Department of Materials and Interfaces, Weizmann Institute of Science, Rehovot, Israel

Abstract

We report on the low frequency tunnel current noise characteristics of an organic monolayer tunnel junction. The measured devices, n-Si/alkyl chain (C₁₈H₃₇)/Al junctions, exhibit a clear $1/f^\gamma$ power spectrum noise with $1 < \gamma < 1.2$. We observe a slightly bias dependent background of the normalized power spectrum current noise (S_I/I^2). However, a local increase is also observed over a certain bias range, mainly if $V > 0.4$ V, with an amplitude varying from device to device. We attribute this effect to an energy-dependent trap-induced tunnel current. We find that the background noise S_I scales with $(\partial I / \partial V)^2$ and a model is proposed which is consistent with our experimental data.

^a Corresponding author : dominique.vuillaume@iemn.univ-lille1.fr

Molecular electronics is a challenging area of research and is envisioned as a complement to usual semiconductor devices.¹ Many works studied the current transport mechanisms² e.g. “through-bond” (through molecules) or “through space” tunneling,^{3,4} and the efficiency of charge transport across the contacts (coupling of molecules to electrodes and density of surface states).⁵ Experimental results mainly concerned dc current (or conductance) versus voltage properties and more recently electron – molecular vibration interactions measured by inelastic electron tunneling spectroscopy.⁶ However, the dc current alone is not sufficient to fully characterize the transport. Current fluctuation phenomena also contain useful physical information. For instance, low frequency I/f noise was used to characterize carrier trapping-detrapping and electrically active defects in classical semiconductor solid-state devices. These measurements still represent a certain challenge in molecular transport experiments mainly due to low currents and sometimes poor reproducibility involved in these experiments. Although some theories about shot noise in molecular systems were proposed,⁷ it is only recently that it was measured, in the case of a single D_2 molecule.⁸ Current noise is often composed of I/f noise at low frequency and shot noise at high frequency. Low frequency I/f noise was studied in thick (multilayer) Langmuir-Blodgett films⁹ and more recently in carbon nanotube transistor,¹⁰ but, up to now, no study of the low frequency current noise in molecular junctions (e.g. electrode/short molecules/electrode) was reported.

Recently, high quality and reproducible alkyl monolayers on oxide-free silicon were reported to be a basic system to study the electrical transport through molecules.¹¹ The thermoionic and tunnel regimes were clearly distinguished depending on the bias voltage. It was also shown that although a combination of characterization techniques is

not sufficient to distinguish between monolayers with minor differences in quality, it appears evident in the current-voltage measurements.¹² Such high quality monolayers allow us to reach the next step in electrical transport, namely the study of noise measurements. Low frequency noise measurements usually allow assessing further information about defects and transport mechanisms.¹³ One can wonder if $1/f$ current noise will be observed in alkyl monolayers. From an application point of view, the study of low frequency noise is required if one consider using these monolayers as ultra-thin gate insulator for nanometer-scale organic transistors,¹⁴ and a comparison with their inorganic counter-part (tunnel SiO_2)^{15,16} is interesting.

We report here, for the first time, the observation and detailed study of the $1/f^\gamma$ power spectrum of current noise through n-Si/ $\text{C}_{18}\text{H}_{37}$ /Al junctions for different forward and reverse biases. We measure and analyse current density - voltage (J - V) curves and confirm the good reproducibility of these organic tunnel junctions. The noise current power spectra (S_I) are measured for different biases. Normalized noise (S_I/I^2 , where I is the dc current) at 10 Hz is plotted and analysed. Superimposed on the background noise, we observe noise bumps over a certain bias range. We propose a model, considering trap-induced tunnel current. We also demonstrate that S_I scales with $(\partial I / \partial V)^2$.

Si-C linked alkyl monolayers were formed on Si(111) substrates (0.05-0.2 $\Omega\cdot\text{cm}$) by thermally induced hydrosilylation of alkenes with Si:H. Sample details are given elsewhere.^{11,12} 50 nm thick aluminium contact pads with different surface areas between $9 \times 10^{-4} \text{ cm}^2$ and $4 \times 10^{-2} \text{ cm}^2$ were deposited at 3 $\text{\AA}/\text{s}$ on top of the alkyl chains. The studied junction, Si-n/ $\text{C}_{18}\text{H}_{37}$ /Al, is shown in Fig.1 (inset). The voltage V is applied to the aluminium pad and the Si is grounded, using a semiconductor signal analyzer Agilent

4155C. Each curve was acquired with a trace-retrace protocol and repeated 3 times with different delay times between each measurement (voltage step $\Delta V=1$ mV) in order to check a possible hysteresis effect and confirm that no transient affects the dc current characteristics. For noise measurements, the experimental setup was composed of a low noise current-voltage preamplifier (Stanford SR570), powered by batteries, and a spectrum analyser (Agilent 35670A). All the measurements were performed under controlled atmosphere (N_2) at room temperature.

Figure 1 shows typical current density – voltage (J - V) curves. We measured 13 devices with different pad areas. The maximum deviation of the current density is about half an order of magnitude. It is interesting to notice that although devices A and C have different contact pad areas (see figure caption), their J - V curves almost overlap. This confirms the high quality of the monolayer. For most of the measured devices, the J - V curves diverge from that of device C at $V > 0.4$ V, with an increase of current that can reach an order of magnitude at 1 V (device B).

Taking into account the difference of work functions between n-Si and Al, considering the level of doping in the silicon substrate (resistivity ~ 0.1 Ω .cm), there will be an accumulation layer in the Si at $V > -0.1$ V.¹⁷ From capacitance-voltage (C - V) and conductance-frequency (G - f) measurements (not shown here), we confirmed this threshold value (± 0.1 V).¹⁸ As a consequence, for positive bias, we can neglect any large band bending in Si (no significant voltage drop in Si). The J - V characteristics are then calculated with the help of the tunnelling Hamiltonian¹⁹ giving

$$J(V) = \frac{emk_B\theta}{2\pi^2\hbar^3} \int_0^{+\infty} dE T(E) \ln\left(\frac{1 + e^{\beta(\mu-E)}}{1 + e^{\beta(\mu-eV-E)}}\right) \quad (1)$$

where e is the electron charge, m the effective mass of the charge carriers within the barrier, k_B the Boltzmann constant, \hbar the reduced Planck constant, μ the Fermi level and $\beta = 1/k_B\theta$ (θ the temperature). $T(E)$ is the transfer coefficient for quasi-electrons flowing through the tunnel barrier with energy E . It is calculated for a given barrier height, Φ , and thickness d and shows two distinct parts: $T(E) = T_1(E) + T_2(E)$. $T_1(E)$ is the main contribution to $T(E)$ that describes transmission through a defect-free barrier. $T_2(E)$ contains perturbative corrections due to assisted tunnelling mechanisms induced by impurities located at or near the interfaces. The density of defects is assumed to be sufficiently low to consider the defects as independent from each other, each impurity at position \vec{r}_i interacting with the incoming electrons via a strongly localized potential at energy U_i , $U_i\delta(\vec{r} - \vec{r}_i)$, The value of U_i is random and considered to be uniformly distributed between 0 and Φ . We write $T_2(E) = \sum_{i=1}^{N_{imp}} T_2(E, U_i)$, with N_{imp} being the number of impurities and $T_2(E, U_i)$ the part of the transmission coefficient caused by the impurity i . The two contributions of $T(E)$ are then calculated exactly following the method of Appelbaum and Brinkman.²⁰ Using Eq. 1, very good agreements with experiments are obtained. As an example, the theoretical J - V characteristic for device C is shown in Fig.1. The best fit is obtained with $\Phi = 4.7$ eV, $m = 0.14 m_e$ (m_e is the electron mass) and 10^{10} traps/cm². The thickness is kept fixed, $d = 2$ nm (measured by ellipsometry).

DC measurements are not sufficient to understand all the fine mechanisms involved in the electrical transport. Low frequency noise is an efficient tool to understand such dispersion effects in J - V curves. For instance, device D shows an anomalous

increase of current (not representative of other devices) starting at $V > 0$ V. Figure 2 shows the low frequency current noise power spectrum S_I for different bias voltages from 0.02 V to 0.9 V. All curves are almost parallel and follow a perfect $1/f^\gamma$ law with $\gamma = 1$ at low voltages, increasing up to 1.2 at 1 V. We could not observe the shot noise because the high gains necessary for the amplification of the low currents induce a cut-off frequency of our current preamplifier lower than the frequency of the $1/f$ – shot noise transition. The $1/f^\gamma$ noise in solid-state devices is now well understood from its microscopic origin, namely random telegraph signal (RTS), each RTS leading to a Lorentzian spectrum. The increase of γ over unity can be attributed to the occurrence of additional RTS behaviour in the tunnelling current at low frequency. Whereas in device C, the increase of γ starts at $V > 0.7$ V, it starts at 0.4 V for device B and γ is equal to 1.2 in all the range [-1 V, 1 V] for device D.

Traps in the tunnel barrier are the most likely cause of the low frequency current noise because traps, or slow states near the interface are one of the few mechanisms that can have carrier capture and emission time constants greater than 10 ms.^{13,21} Fluctuations in current are attributed to fluctuations in the electron density at the interface due to trapping. The increase of γ up to 1.2 above a certain bias leads us to consider that additional traps exist at certain energies. This is discussed later, in correlation with a model.

In most devices, the low frequency $1/f$ current noise usually scales as I^2 , where I is the dc tunnel current.^{16,21} This normalization provides information about the signal to noise ratio. In Fig.3, we present the normalized current noise power spectrum S_I/I^2 at 10 Hz (it is customary to compare noise spectra at 10 Hz) as a function of the bias V for

devices B, C and D. Device C has a basic characteristic with almost all points following the dashed line asymptote. Therefore, we use it as a reference for comparison with other devices. One can note that basically, devices B, C and D have the same tendency, following this guide. S_I/I^2 decreases exponentially with $|V|$ as observed previously in inorganic (SiO_2) tunnel junctions. However, in the case of organic alkyl chains, we observe a local (Gaussian with V) increase of noise at $V > 0.4$ V for most samples (shown here for devices B and C). The amplitude of the local increase varies from device to device. This local increase of noise is correlated with the increase of current seen already in the J - V curves. The J - V characteristics of device B diverge from those of device C at $V > 0.4$ V and this is consistent with the local increase of noise observed in Fig.3. Even in the case of an atypical device such as D, the local increase of noise (at $V > 0$ V) and high currents are linked. The current I can be considered as a sum of a noise-free tunnel current I_0 and a trap assisted tunnel current I_T . At $V > 0$, traps in the tunnel barrier with an energy below the Si CB and above the metal Fermi level contribute to the noise. At $V < 0$, traps above the Si-CB and below the metal Fermi level are contributing. Thus, the observed excess noise bump at $V > 0$ may be attributed to a larger density of traps above the metal Fermi level than below. Neglecting any voltage drop in the silicon, the highest trap density is located at the energy $0.4 < E < 1$ eV within the alkyl energy gap above the Fermi level position of aluminum. The nature and origin of these traps is not known. From J - V curves and S_I/I^2 , the trap-induced tunnel current may be significant in the total tunnel current when $S_I/I^2 @ 10$ Hz is over 10^{-6} Hz^{-1} .

To model the tunnel current noise in the monolayers, we assume that some of the impurities may trap charge carriers. Since we do not know the microscopic details of the

trapping mechanisms and the exact nature of these defects, we associate to each of them an effective Two-Level Tunnelling Systems (TLTS) characterized by an asymmetric double well potential with the two minima separated in energy by ε_i . We denote as Δ_i the term allowing to tunnel from one well to the other, and get after diagonalization two levels distant in energy by $E_i = \sqrt{\varepsilon_i^2 + \Delta_i^2}$. The lower state (with energy E_i^-) corresponds to an empty trap, the upper state (with energy E_i^+) to a charged one. The relaxation rate from the upper to the lower state should be determined by the coupling with the phonons and with the tunnelling quasi-electrons. In all cases, the time scale of the relaxation, τ , is very long compared to the duration of a scattering event. This allows us to consider the TLTS with a definite value at any instant of time. We then get the following spectral density of current for each TLTS²²

$$S_i^i(f) = \overline{(I_- - I_+)^2} \frac{\tau}{1 + \varpi^2 \tau^2} \text{Cosh}^{-2} \frac{E_i}{2k_B \theta} \quad (2)$$

where $\varpi = 2\pi f$ and $I_{-(+)}$ is the tunnel current for the empty (charged) impurity state. In this equation the average of $(I_- - I_+)$ over the TLTSs having similar ε_i and Δ_i is taken. The difference between the two levels of current has two different origins. The first one is the change in energy of the impurity level that directly affects $T_2(E)$. The second one is the change in the charge density at the interfaces of the molecular junction induced by the trapped quasi-electron that produces a shift in the applied bias, δV . We write

$$I_+(V) \cong I_-(V + \delta V) + A \frac{emk_B \theta}{2\pi^2 \hbar^3} \int_0^{+\infty} dE \frac{\partial T_2(E, U_i)}{\partial U_i} \Big|_{E_i^-} E_i \ln \left(\frac{1 + e^{\beta(\mu - E)}}{1 + e^{\beta(\mu - eV - \delta V - E)}} \right) \quad (3)$$

where A is the junction (metal electrode) area. The first term in the right hand side is due to the fluctuating applied bias, the second to the change in impurity energy. Since $T_2(E)$ is already a perturbation, the second contribution is smaller than the first one and is neglected in the following. Moreover, we assume for simplicity that all the charged impurities give the same shift of applied bias and take $\delta V = e / C_{TJ} A$, where C_{TJ} is the capacitance of the tunnel junction per unit surface, which is observed to be almost constant for positive bias. By using the usual approximation regarding the distribution in relaxation times, τ , and energies, E_i , we finally get²²

$$S_I \propto E^* \frac{1}{A} N_{imp}^* \left(\frac{\partial I}{\partial V} \Big|_- \right)^2 \frac{e^2}{C_{TJ}^2} \frac{1}{f} \quad (4)$$

We assume, in particular, the energy distribution of impurities to be uniform to get the $1/f$ dependence. In this last expression, the derivative of the current is evaluated for the lower impurity state, N_{imp}^* is the impurity density by energy and surface unit. E^* is the mean value of E_i that should be replaced by $k_B \theta$ at low temperatures. It is important to stress that N_{imp} can not be determined accurately from the last equation because of lack of information concerning the microscopic nature of the traps.

We confirm this predicted dependence of S_I on $(\partial I / \partial V)^2$, a dependence already stressed in studies of ultra thin gate oxides.¹⁵ In Fig.4, S_I vs. $(\partial I / \partial V)$ is plotted on a log-log scale for device C. We clearly identify a slope 2. At the same time (see inset), it is very interesting to notice that $S_I - I$ also follows a power law with a slope of 1.7 and not 2 as supposed. The value $1.7 < 2$ explains why the normalized noise S_I / I^2 decreases with V (Fig. 3). The appropriate normalization factor to obtain flat background noise is $S_I / I^{1.7}$.

These two features imply that $(\partial I / \partial V)^2$ scales with $I^{1.7}$ which has been experimentally verified from the I - V curves (not shown). The local increases, seen in Fig. 3, can be explained by assuming additional traps with appropriate energies. These traps give a non-uniform contribution to the energy distribution of defects that breaks the I/f dependence of S_I above certain bias. This is indeed what is observed in Fig. 2.

In summary, our study show that the low frequency current noise (I/f^γ) is a very sensitive tool to characterize defects in molecular junctions such as Si/C₁₈H₃₇/Al. We could correlate the small dispersion observed in dc J - V characteristics and the local increase of normalized noise at certain biases (mainly at $V > 0.4$ V). The power spectrum of the background current noise is proportional to $(\partial I / \partial V)^2$ as expected from theory. We also show that the power spectrum of the current noise should be normalized as $S_I/I^{1.7}$.

We are indebted to David Cahen for his support and great interest on this work and very valuable discussions in several occasions. We acknowledge IRCICA and CNRS through "ACI nanosciences" project Nanosys (n° 04 2 320) for a partial financial support. N.C. and S.P. thank the "ACI nanosciences" program and IRCICA for post-doc grants, respectively. We thank Hiroshi Inokawa, Frederic Martinez for helpful comments.

Captions:

Fig.1: Experimental J - V curves at room temperature for n-Si/C₁₈H₃₇/Al junctions. The contact areas are 0.36 mm² for device A and 1 mm² for devices B, C and D. Device D shows an anomalous increase of current. 11 of the 13 devices measured show electrical characteristic between those of devices C and D.

Fig.2: Low frequency (I/f^γ) power spectrum current noise for device C. Although we measured all spectra of the sequence $|V|=[0.02; 0.05; 0.1; 0.15; 0.2; 0.25; 0.3; 0.35; 0.4; 0.45; 0.5; 0.6; 0.7; 0.8; 0.9; 1 \text{ V}]$, we selected for this figure only spectra with $V > 0 \text{ V}$ and a spacing of 0.2 V for clearer presentation. γ varies from 1 at low voltages to 1.2 at 1 V.

Fig.3: Normalized power spectrum current noise S_I/I^2 as a function of bias V for devices B, C and D. The curve for device C follows asymptotes (dashed lines) which are used as a reference for other devices. A local increase of noise over the asymptotes with a Gaussian shape is shown.

Fig.4: $S_I - (\partial I/\partial V)$ curve for device C on a log-log scale. The dashed line represents the slope of 2. In the inset, the $S_I - I$ curve is also presented on a log-log scale with a slope of 1.7.

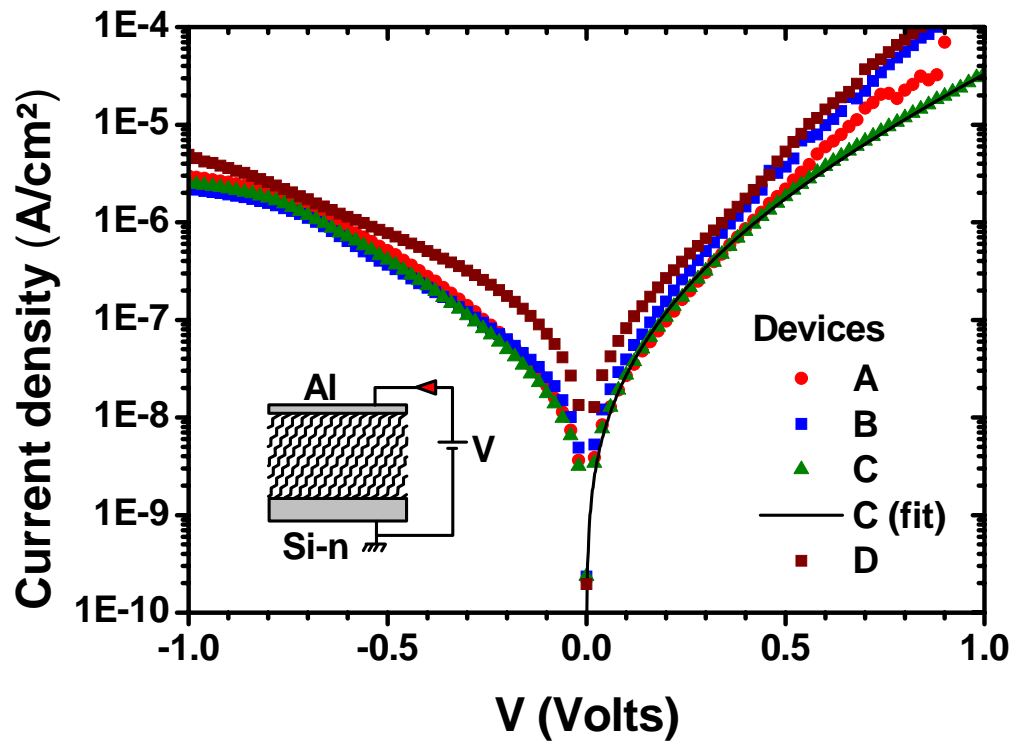


Figure 1

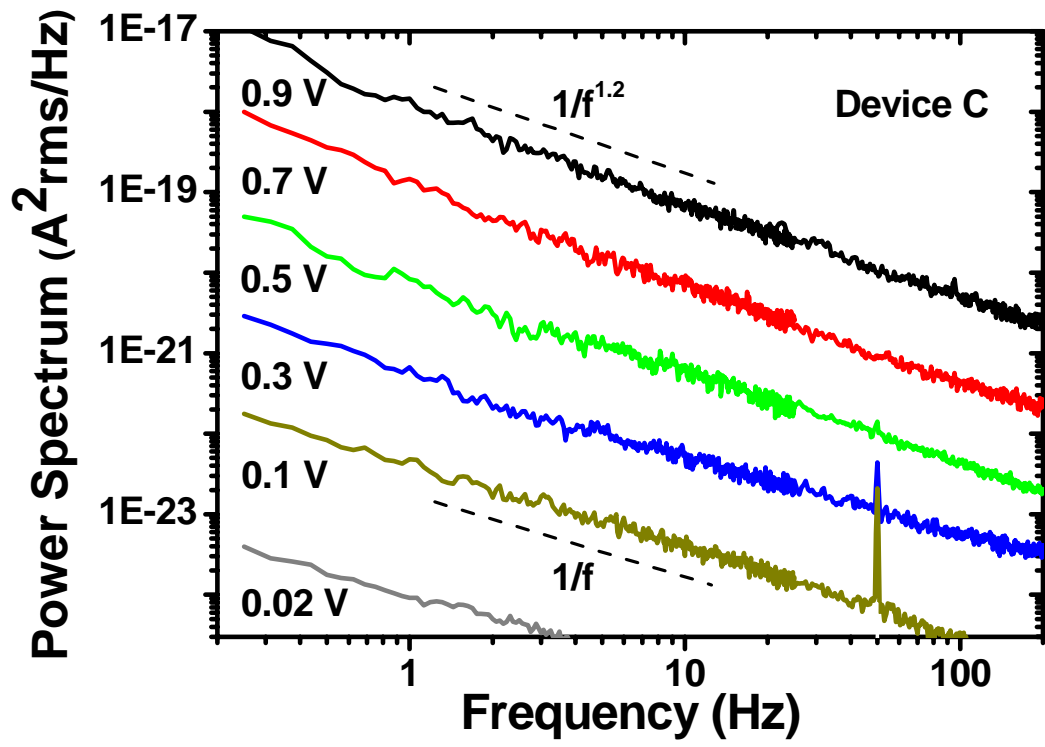


Figure 2

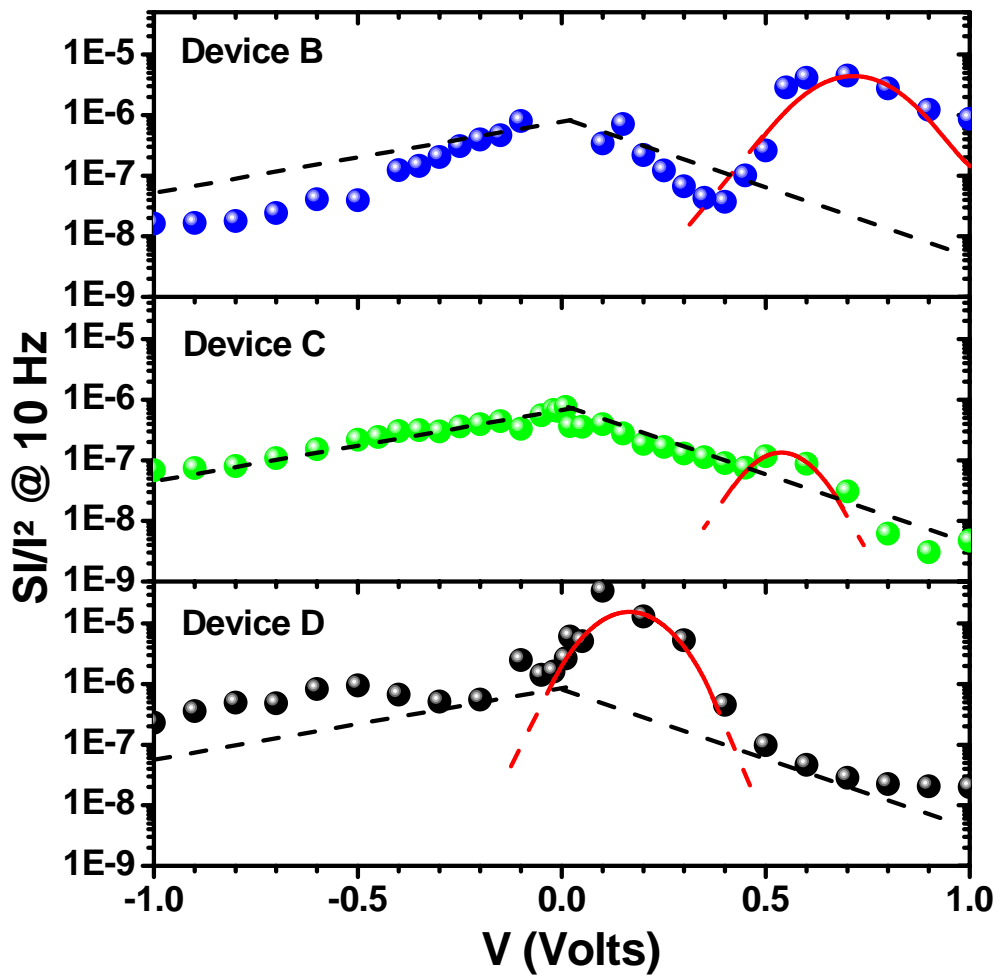


Figure 3

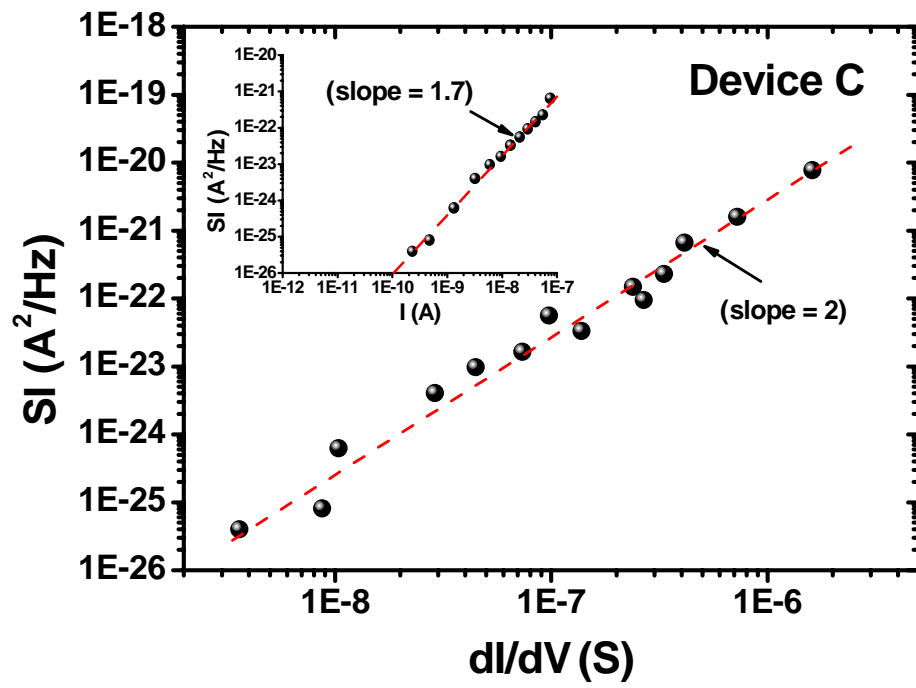


Figure 4

-
- ¹ A. Aviram and M. A. Ratner, Chem. Phys. Lett. **29**, 277 (1974).
- ² A. Nitzan and M. A. Ratner, Science **300**, 1387 (2003).
- ³ A. Salomon, D. Cahen, S. Lindsay, J. Tomfohr, V. B. Engelkes, and C. D. Frisbie, Adv. Mater. **25**, 1881 (2003).
- ⁴ K. Slowinski, R. V. Chamberlin, C. J. Miller, and M. Majda, J. Am. Chem. Soc. **119**, 11910 (1997).
- ⁵ V. V. Zhirnov and R. K. Cavin, Nature Mat. **5**, 11 (2006).
- ⁶ W. Wang, T. Lee, I. Krestchmar, et al., Nano Lett. **4**, 643 (2004); J. G. Kushmerick, J. Lazorcik, C. H. Patterson, et al., Nano Lett. **4**, 643 (2004); A. Troisi and M. A. Ratner, Phys. Rev. B **72**, 033408 (2005); D. K. Aswal, C. Petit, G. Salace, et al., Phys. Stat. Sol. (a) **203**, 1464 (2006); C. Petit, G. Salace, S. Lenfant, et al., Microelectronic Engineering **80**, 398 (2005).
- ⁷ M. Galperin, A. Nitzan, and M.A.Ratner, Phys. Rev. B. **74**, 075326 (2003); A. Thielmann, M.H. Hettler, J. König, and G. Schön, Phys. Rev.B . **68**, 115105 (2003); A. Thielmann, M.H. Hettler, J. König, and G. Schön, Phys. Rev. Lett. **95**, 146806 (2005); R. Guyon, T. Jonckheere, V. Mujica, A. Crépieux, and T. Martin, J. Chem. Phys. **122**, 144703 (2005).
- ⁸ D. Djukic and J.M. van Ruitenbeek, Nano Letters **6**, 789 (2006).
- ⁹ L.A. Galchenkov, S.N. Ivanov, I.I. Pyataikin, V.P. Chernov and P. Monceau, Phys. Rev. B, **57**, 13220 (1998); S. Malik, A.K. Ray and S. Bruce, Semicond. Sci. Technol. **20**, 453 (2005).

-
- ¹⁰ P.G. Collins, M.S. Fuhrer, A. Zettl, Appl. Phys. Lett. **76**, 894 (2000); Y.-M. Lin, J. Appenzeller, J. Knoch, Z. Chen and P. Avouris, Nano Letters **6**, 930 (2006).
- ¹¹ A. Salomon, T. Boecking, C.K. Chan, F. Amy, O. Girshevitz, D. Cahen, and A. Kahn, Phys.Rev.Letters **95**, 266807 (2005).
- ¹² O. Seitz, T. Böcking, A. Salomon, J.J. Gooding, and D. Cahen, Langmuir **22**, 6915 (2006).
- ¹³ M.J. Kirton and M.J. Uren, Adv. in Physics, **38**, 367 (1989).
- ¹⁴ J. Collet and D. Vuillaume, Appl. Phys. Lett. **73**, 2681 (1998); J. Collet, O. Tharaud, A. Chapoton and D. Vuillaume. Appl. Phys. Lett. **76**, 1941 (2000).
- ¹⁵ F. Martinez, S. Soliveres, C. Leyris, and M. Valenza, IEEE ICMTS Proceedings, 193 (2006).
- ¹⁶ G.B. Alers, K.S. Krisch, D. Monroe, B.E. Weir and A.M. Chang, Appl. Phys. Lett. **69**, 2885 (1996).
- ¹⁷ S.M. Sze, *Physics of Semiconductor Devices* (Wiley, New York, 1981)
- ¹⁸ N.Clement, S.Pleutin, O.Seitz, S.Lenfant, D.Cahen and D.Vuillaume, in preparation.
- ¹⁹ G.D. Mahan, *Many-Particle Physics*, 3rd Ed. (Plenum, New York, 2000).
- ²⁰ J.A. Appelbaum and W.F. Brinkman, Phys. Rev. **B 2**, 907 (1970); more details about the calculation of $T(E)$ will be given in Ref. 18.
- ²¹ C.T. Rogers and R.A. Buhrman, Phys. Rev. Lett. **53**, 1272 (1984)
- ²² S.M. Kogan, *Electronic noise and fluctuations in solids*, (Cambridge University Press, 1996).